CROATICA CHEMICA ACTA CCACAA **65** (2) 327–344 (1992)

ISSN 0011-1643
UDC 541.1
CCA–2062

Original Scientific Paper

Phase Transitions in Microconfined Nematic Liquid Crystals

Marija Vilfan

J. Stefan Institute, University of Ljubljana, Jamova 39, Ljubljana, Slovenia

and

Slobodan Žumer

Department of Physics, University of Ljubljana, Jadranska 19, Ljubljana, Slovenia

Received November 25, 1991

A brief review of stable phases and phase transitions in microconfined nematic liquid crystals is given. The effects of confinement are studied for the cavities of spherical and cylindrical shape with different surface-liquid crystal interactions. The phase transitions are either of order-disorder type where the magnitude of orientational ordering changes or of the structural type between different configurations of the nematic director field.

GENERAL CONSIDERATIONS

The basic characteristic of liquid crystals is their long-range orientational molecular order.[1] It is generally described by a second-rank symmetric tensor $\boldsymbol{Q}_{ij}$.[1,2] In the phases with local uniaxial symmetry, $\boldsymbol{Q}_{ij}$ can be expressed in terms of a scalar order parameter and a vector field. The order parameter S describes the magnitude of the orientational order, and the unit vector, called the director $\vec{n}$, points along the local ordering direction:

$$\boldsymbol{Q}_{ij} = \frac{1}{2} S(3n_i n_j - \delta_{ij}) \,. \tag{1}$$

In the limit of infinitely large, spatially homogeneous systems the value of S is zero in the isotropic phase and different from zero in the nematic phase. The phase transition, which occurs at a well defined temperature T_c, is weakly first order. Therefore the Landau theory,[3] modified by de Gennes,[4] is appropriate for its description.[1,2]

However, in the practical circumstances, the ideal configuration of the system with spatially uniform S and $\vec{n}$ is hardly realized because of constraints which are imposed by the limiting surfaces of the sample or by external electric or magnetic field acting on the molecules. The deformed configuration results as a balance of surface forces,

elastic forces and external-field interactions. If the spatial variations occur over distances which are much larger than molecular dimension, the local properties are still those of a uniaxial liquid crystal, but the order parameter is space-dependent:

$$Q_{ij}(\vec{r}) = \frac{1}{2} S(\vec{r}) \left[3n_i(\vec{r}) n_j(\vec{r}) - \delta_{ij}\right] . \tag{2}$$

Describing the phase transitions in the confined nematic liquid crystals, we use the word »phase« in its generalized sense meaning an equilibrium state with a certain spatial distribution of the orientational ordering of molecules. The phase transitions can be thus classified into two types: *order-disorder phase transitions* between phases with a different magnitude of orientational order, and *structural phase transitions* between different director fields (configurations) within the nematic phase. Both types have been studied first in planar geometry (liquid crystal between two flat, parallel plates)[5] which is the simplest choice for microscopic observations and is used also in the liquid crystal display (LCD) cells.

Order-Disorder Phase Transitions (isotropic to nematic and nematic to the crystalline or smectic phases) are induced by changing the temperature. The pressure effects are here neglected. This type of phase transitions is characterized mainly by the discontinuity of the magnitude of the order parameter $S(\vec{r})$.

The isotropic-nematic transition in thin planar films was theoretically studied in detail by Sheng.[5] He revealed a number of new phenomena, not present in macroscopic liquid crystal samples, but appearing when a nematic liquid crystal is at least in one dimension confined to micron sizes. He showed that:

– In a finite-thickness sample and at finite temperature the liquid-crystal exhibits a certain, though small, degree of surface-induced orientational order in the whole sample even in the high temperature phase, which is therefore called »paranematic« instead of isotropic.

– The paranematic-nematic transition temperature T_c is characterized by an abrupt change of the order parameter value in the central part of the sample. T_c increases with decreasing thickness of the sample within the interval of 0.5 K. It was shown later that also a decrease in the transition temperature can take place if the confining surface induces disorder instead of order.[6]

– For nonzero values of the surface-liquid crystal interaction potential the paranematic-nematic coexistence curve terminates at a critical sample thickness in a critical point. Below this critical thickness there is a continuous decrease of order upon heating with no phase transition.

–Close to the solid-liquid crystal interface a boundary layer exists where the degree of the orientational order can differ significantly from that of the interior of the sample.

– For limited values of the substrate-liquid crystal interaction potential and a certain range of sample thicknesses there is a phase transition which takes place only in the boundary7 layer and occurs at temperatures slightly above the nematic-to-paranematic transition (»boundary-layer phase transition«).

Structural Phase Transitions between different director configurations within the nematic phase occur below the nematic-paranematic transition temperature. They are induced either by external field, by the temperature which changes elastic constants

and surface anchoring, or by a mechanical stress which deforms the confining cavity. The characteristic feature of this kind of phase transitions is the discontinuous change of the director field $\vec{n}(\vec{r})$, while the magnitude of the order parameter is to a good approximation constant and unaffected throughout the most of the sample except in the vicinity of defects.

Freedericksz was the first to observe this type of phase transition under microscope.[7] He pointed out that the liquid crystal oriented perpendicularly between two glassy plates remains unperturbed only up to a certain critical value of the magnetic field B_c which is applied parallel to the plates. For higher values the equilibrium configuration corresponds to the state with molecules aligned along the magnetic field in most of the slab except for two thin layers near each wall. The phase transition between the unperturbed configuration and the distorted configuration, which takes place at the critical value B_c, is of second order, and the distortion just above the threshold very small. The critical value of the magnetic field B_c is given by

$$B_c = \frac{\pi}{d}\sqrt{\mu_0 K_3/\chi_a} \tag{3}$$

where d is the sample thickness, K_3 one of the elastic constants appropriate for the geometry described above, and χ_a the diamagnetic anisotropy of the liquid crystal. Observations of the Freedericksz transitions in different conditions allow a simple determination of all three nematic elastic constants.

In this paper we give a short review of phase transitions which occur in a nematic liquid crystal confined into spherical and cylindrical microcavities within a solid polymer. This type of materials, called PDLC (Polymer Dispersed Liquid Crystals) has been only recently discovered.[8] In their most common form they consist of micron-size droplets of a low-molecular-weight nematic liquid crystal dispersed in a polymer binder. PDLC materials containing nematic droplets with more or less *spherical shape* and radius ranging from 0.1 μm to $\sim 10^2$ μm are produced by a polymerization-induced phase separation of the liquid crystal and polymer binder.[9] Droplet size and morphology depend on the speed of the droplet nucleation and gelation of the polymer. Phase separation can be also induced thermally by a controlled cooling of a solution of liquid crystal and a thermoplastic polymer (heated above the melting temperature).[9] The uniformity of the droplet sizes can be well illustrated by a scanning-electron-microscope image of a cut through a PDLC material (Figure 1).

Micron-size nematic droplets strongly scatter light and the PDLC material has an opaque white appearance. The application of an appropriate external electric field induces a phase transition accompanied by a substantial change of liquid crystal ordering in the droplets which causes a large change in the light scattering from the dispersion.[10] A PDLC film, initially opaque, becomes transparent when an appropriate electric field is applied to a material with ordinary refractive index of the liquid crystal matched to the index of the polymer. This simple electrooptic effect is the physical base for the operation of new PDLC based liquid crystal displays, appropriate particularly for the video-projection systems, optical processing devices and large switchable windows.[11,12]

The preparation of the liquid crystal in open *cylindrical cavities* offers a more direct control of the geometry and surface interaction. Besides capillary glassy tubes, which can be made with diameters as small as a few micrometers, organic membranes with submicrometer cylindrical cavities were discovered recently. Such cavities appear

in organic polymer membranes after ionic bombardment perpendicular to the membrane and appropriate etching. The resulting cavities can be filled with the nematic liquid crystal[13,14] like capillary glassy tubes. The walls of open cylindrical cavities can be previously treated by a suitable surfactant to achieve the desired type and strength of the surface interaction. This enables indirect studies of liquid crystal material constants. Recently, an analogy was shown between the nematic defects and cosmic strings extending thus the problem of nematic structures far beyond the borders of the condensed matter physics.[15] In contrary to PDLC materials, the cylindrically microconfined liquid crystals are so far of small practical importance except for the modelling of liquid crystal optical wave guides.[16]

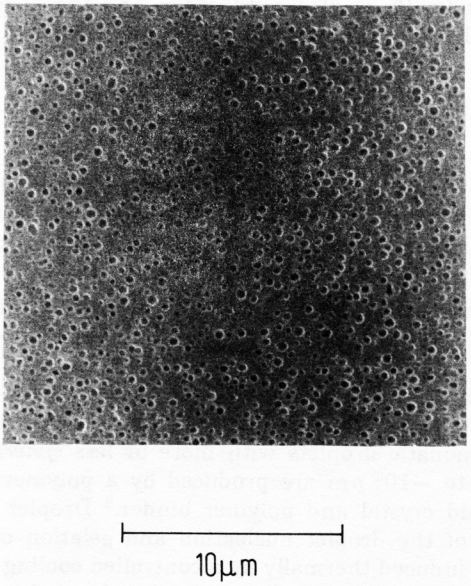

Figure 1. Scanning-electron-microscope photograph of a nematic liquid crystal microdroplet dispersion (cross-cut of the PDLC material) made at the Liquid Crystal Institute, Kent State University, Kent, Ohio.

In the last year, gels with polymer networks in liquid crystals have been reported as potential candidates for electrooptic application as well.[17,18] In these materials, a small percentage of the polymer forms an irregular, fractal-like network which constrains the liquid crystal into microcavities of varying size and shape. So far there is hardly any information about the possible structures of such volume-stabilized liquid crystal materials and for this reason they are not included in the present review.

In this paper we will present only the most basic features of nematic liquid crystals confined into spherical and cylindrical microcavities. Several simplifications will be introduced in order to give an insight into the subject also for non-specialists in the field.

THEORETICAL APPROACH

In the phenomenological approach, the stable phases and configurations of microconfined liquid crystals are theoretically determined by finding the structures which have the minimum free energy. To obtain the free energy of a liquid crystal in a cavity, the Landau-de Gennes approach based on the expansion in terms of the order parameter is usually used.[1-4] The free energy density

$$f(\vec{r},T) = f_h + f_n + f_s + f_f \tag{4}$$

consists of four parts: the homogeneous, but temperature dependent f_h, corresponding to a non-distorted bulk nematic liquid crystal; the spatially inhomogeneous part f_n; the part arising from the surface interactions at the cavity wall f_s; and the interaction with an external electric or magnetic field f_f.

The homogeneous part f_h, expressed in terms of S up to the fourth power, is

$$f_h = f_o + \frac{1}{2}a(T - T^*)S - \frac{1}{3}BS^3 + \frac{1}{4}CS^4 \ , \tag{5}$$

where the coefficients a, B and C are positive and temperature independent material constants. T^* is the supercooling limit of the bulk isotropic phase.

The spatially inhomogeneous part f_n includes spatial derivatives of S and $\vec{n}$. Including only terms up to the second order in derivatives of the director field and order parameter and taking into account the symmetry requirements, one obtains:

$$f_n = \frac{1}{2}[K_{11}(\operatorname{div}\vec{n})^2 + K_{22}(\vec{n}\cdot\operatorname{rot}\vec{n})^2 + K_{33}(\vec{n}\times\operatorname{rot}\vec{n})^2 - \\ - K_{24}\operatorname{div}(\vec{n}\times\operatorname{rot}\vec{n} + \vec{n}\cdot\operatorname{div}\vec{n})] + \frac{3}{4}L_1(\vec{\nabla}S)^2 \ . \tag{6}$$

Here K_{11} denotes the elastic constant for splay deformation, K_{22} for the twist, K_{33} the bend elastic constant, and K_{24} the saddle-splay constant which characterizes the so-called surface elastic free energy. In a nematic liquid crystal all elastic constants K_i are of the same order of magnitude and proportional to the square of the order parameter S. L_1 is a temperature independent constant with a value comparable to the above elastic constants.

The surface-interfacial interaction term f_s is usually described by a simple expression:

$$f_s = -g + \frac{1}{2}w_o \sin^2(\theta_o - \theta) \ , \tag{7}$$

where g measures the isotropic and w_o the anisotropic part of the interfacial liquid crystal-polymer interaction. g and w_o are proportional to the magnitude of the order parameter S. w_o is usually called the directional anchoring strength. θ_o and θ are the preferred and the actual anchoring angles of liquid crystal molecules at the wall.

The contribution f_f to the free energy density, which arises from the coupling of the director with the external magnetic or electric field, depends partly on the orientation of the director:

$$f_{f,B} = -\frac{1}{2}\frac{\chi_a}{\mu_o}(\vec{n}\cdot\vec{B})^2 \,. \tag{8}$$

Here B is the magnetic flux density and χ_a the anisotropy of the diamagnetic susceptibility. The magnetic coherence length $\xi(B)$

$$\xi(B) = \sqrt{\mu_o K_i/\chi_a}\ \frac{1}{B} \tag{9}$$

is a measure for the effect of the magnetic field on the nematic liquid crystal strongly anchored to the confining surface. The magnetic field strongly influences the structure on distances larger than the coherence length. The magnetic coherence length of the liquid crystal 4'-n-pentyl-4-cyanobiphenyl (5CB) is ~7 μm in the field 1 T requiring cavities with $2R >$ · · μm in order to study the magnetic field effects.

In the case of applied electric field E, the orientationally dependent contribution to the free energy density is:

$$f_{f,E} = -\frac{1}{2}\varepsilon_o \Delta\varepsilon\,(\vec{n}\cdot\vec{E})^2 \,, \tag{10}$$

where $\Delta\varepsilon$ denotes the anisotropy of the static dielectric constant. The comparison of the relative efficiencies of the magnetic and electric field shows that 10 kV/cm is roughly equivalent to 1 T.

The minimization of the total free energy of the liquid crystal, *i.e.* of the volume integral $\int (f_h + f_n + f_s + f_f)\,dV$ over the whole cavity, is used for the determination of possible stable and metastable structures. This procedure which should be done numerically in most cases[19,20] is performed either directly or by solving the corresponding Euler-Lagrange differential equations to obtain $S = S(\vec{r},T)$ and $\vec{n} = \vec{n}(\vec{r},T)$.

The procedure can be simplified when certain conditions are met. In the case of strong anchoring at the surface, when the actual angle of director at the surface equals the one preferred by the wall, both interfacial and elastic surface terms vanish. In the intermediate vicinity of the nematic-isotropic phase transition only the terms with $S(\vec{r},T)$ are important, which allows us to neglect the terms with $\vec{n}$. On the other hand, at temperatures far from the phase transition, S can be considered to be spatially independent, except very close to the defects, and only the terms including the elastic deformations of the director field are important to determine the stable configuration.

Some theoretical and experimental results concerning the ordering, stability, and phase transitions in microconfined nematic liquid crystals are presented in the Results and Discussion sections.

SPHERICAL DROPLETS – RESULTS AND DISCUSSION

Among many possible stable configurations, *i.e.* director fields, of a nematic liquid crystal in a spherical microcavity, two relatively simple are usually met: the *radial* director field (Figure 2a), where the molecules are anchored perpendicular to the droplet wall, and the *bipolar* director field (Figure 2c), which can occur when the elongated molecules of the nematic liquid crystal are anchored tangentially to the wall. The radial configuration possesses only the splay-type deformation with a point defect at

the center, called the hedgehog. The bipolar structure is characterized by the presence of two point defects at the poles of the droplet (boojums). The bipolar structure occurs in most PDLC materials produced for practical purposes.

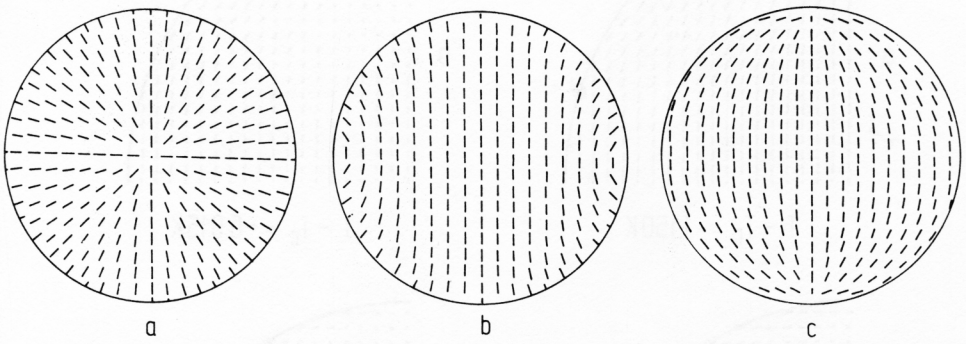

Figure 2. Schematic presentation of the director field in the meridial plane of a spherical droplet for: (a) radial structure, (b) axial structure, (c) bipolar structure.

The Order-Disorder Phase Transitions – Spherical Droplets

The order-disorder phase transition from the disordered, high temperature phase into the nematic phase has been theoretically investigated for the radial[21] and bipolar[19] structure and experimentally for the latter.[22] In the first step of investigation *strong anchoring condition* (w_o, $g \to \infty$) at the droplet wall is assumed, where the constant anchoring angle and constant value of the surface order parameter S_o are maintained. The results are similar for bipolar and radial configurations.

The changes in the nematic ordering close to the phase transition from the ordered, low temperature phase into the high temperature phase are shown in Figure 3 for the bipolar structure.[19] The magnitude of the order parameter S is represented by the length of the bars which indicate the preferred molecular orientation in a meridial cross-cut of the droplet. In the ordered, nematic phase, at least 1 K below the transition temperature, the order parameter is nearly constant throughout the droplet except close to the defect regions at poles which are relatively small (Figure 3a). As the transition temperature is approached from below (or the droplet radius is decreased) the defect regions extend to a much larger part of the volume. Besides, the center of the defect moves towards the inside of the droplet (Figure 3b) which is the consequence of somewhat artificial boundary condition. The first order phase transition from the low temperature into the high temperature phase occurs at the temperature T_c where the free energies of the two phases are equal. It is accompanied by a discontinuous decrease of the order parameter in the center of the droplet (Figure 3c). As the temperature is further increased the liquid crystal material in the microcavity – in contrast to macroscopic bulk samples – retains a small degree of the orientational order within the whole volume (Figure 3d). The high temperature phase is therefore called paranematic phase instead of isotropic. The orientational order is increased in a thin layer at the surface (Figure 3d).

The behavior of the order parameter in the center of the droplet, $S(0)$, reveals the nature of the phase transition. As shown in Figure 4a the first order transition takes

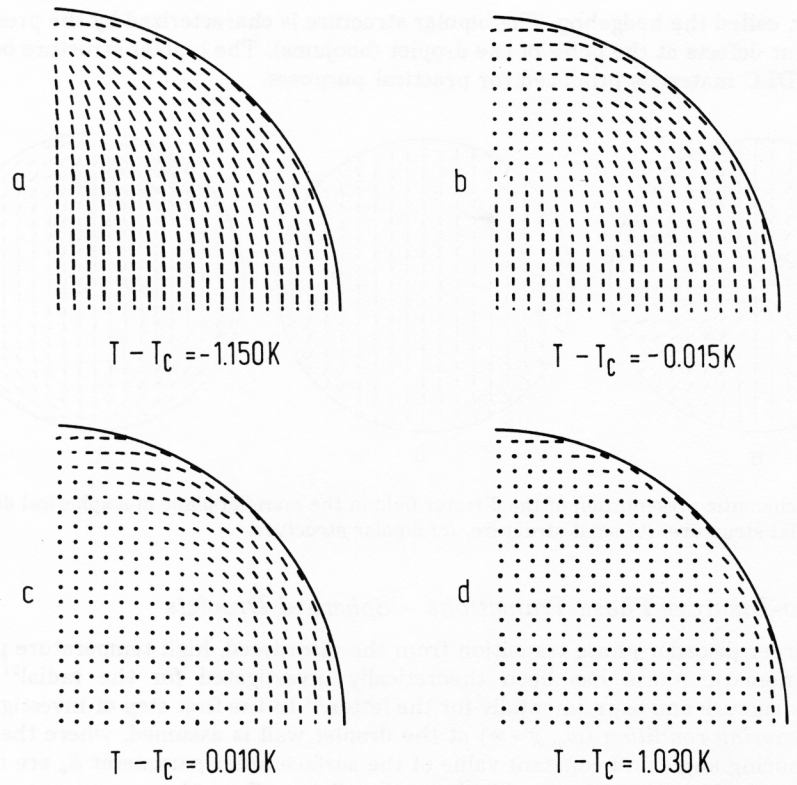

Figure 3. Computer simulation of the nematic ordering in a microdroplet with bipolar structure in the vicinity of the nematic-paranematic phase transition (after Ref. 19.) The orientation of the bars represents the director orientation and their length the magnitude of the order parameter.

place only for large radii. Below a critical radius R_c, the transition disappears and the ordering is completely controlled by the surface. The degree of order in the interior of the droplet decreases continuously as the temperature increases. The critical radius for the 5 CB liquid crystal and strong surface anchoring is 0.067 μm for the droplets with bipolar structure[19], and 0.22 μm for radial structure[21], which is considerably more than 0.02 μm reported for the planar geometry.[5]

The paranematic-nematic transition temperature equals the bulk transition temperature in large droplets with radius $> \sim 10\,\mu$m. With decreasing radius the transition temperature slightly increases because the surface ordering promotes the nematic phase. With further decrease of the radius, however, the free energy of the nonuniform director field causes a decrease in the transition temperature below the value of the bulk sample, which was not observed in the planar geometry. The differences between the bulk and microconfined liquid crystal transition temperatures are rather small, smaller than 0.1 K.

The theoretical predictions of molecular ordering close to the nematic-paranematic phase transition in bipolar nematic droplets were tested experimentally by optical

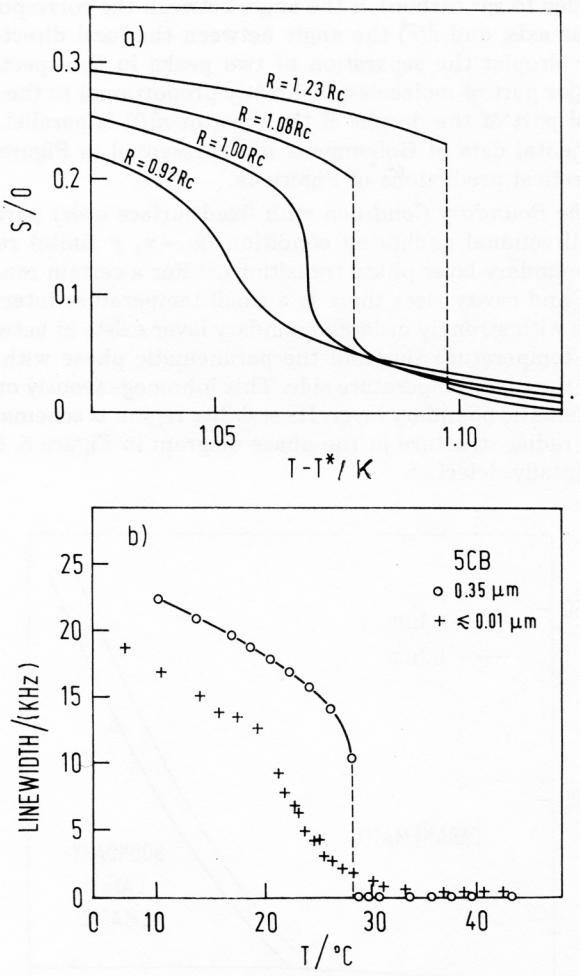

Figure 4. Theoretical (a) and experimental (b) temperature dependence of the order parameter S in the center of the droplet with bipolar structure. Experimental data are taken from Ref. 22.

microscopy in supramicron droplets, and by calorimetric studies and deuterium nuclear magnetic resonance (NMR) in submicrometer droplets where the most interesting processes take place.[22] The NMR spectrum of deuterium nuclei provides a direct insight into the ordering in the droplet as the quadrupole splitting of resonance lines arising from the droplet region with positional vector $\vec{r}$, $\Delta\nu_q(\vec{r})$ depends directly on the local preferred molecular direction $\vec{n}(\vec{r})$ and on the magnitude of orientational order $S(\vec{r})$.[23]

$$\Delta\nu_q(\vec{r}) = \frac{3}{8} C(3\cos^2\alpha - 1)(3\cos^2\vartheta(\vec{r}) - 1) S(\vec{r}) \quad , \tag{11}$$

with C being the static quadrupole coupling constant of deuterium nuclei (~170 kHz for deuterons bonded to sp^3 carbon), α the angle between the corresponding C–D bond and long molecular axis, and $\vartheta(\vec{r})$ the angle between the local director and magnetic field. In a bipolar droplet the separation of two peaks in the spectrum, which correspond to the major part of molecules, is directly proportional to the order parameter $S(0)$ in the central part of the droplet if the director $\vec{n}(0)$ is parallel to the magnetic field. The experimental data of Golemme *et al.*[22] presented in Figure 4b, confirm excellently the theoretical predictions of Figure 4a.

Releasing of the Boundary Condition with fixed surface order parameter value but retaining strong directional anchoring condition ($w_0 \to \infty$, g finite) results in the appearance of the »boundary layer phase transition«.[21] For a certain range of the surface coupling potential and cavity sizes there is a small temperature interval in which the paranematic phase with strongly ordered boundary layer exists in between the nematic phase on the low temperature side and the paranematic phase with weakly ordered boundary layer on the high temperature side. This inhomogeneously ordered phase has a relatively large nematic boundary layer. Its stability region is schematically presented for a droplet with radial structure in the phase diagram in Figure 5. So far it has not yet been experimentally detected.

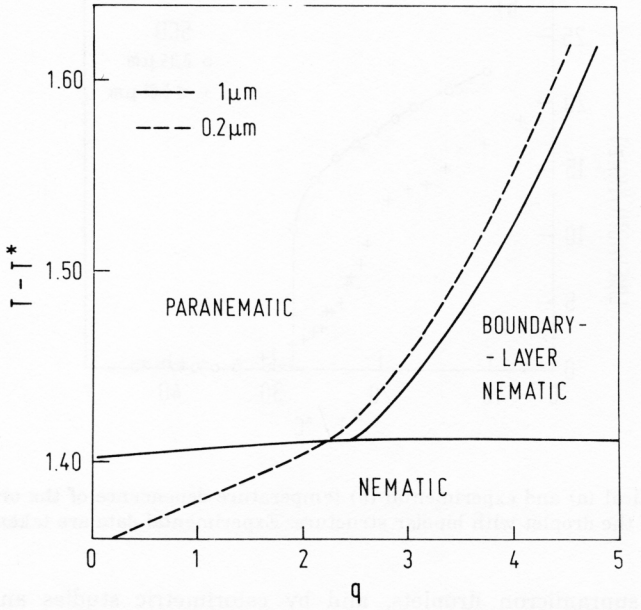

Figure 5. The phase diagram for the paranematic, boundary-layer nematic and nematic phase in a droplet with radial structure for two droplet radii (after Ref.21). The solid line is plotted for a droplet radius larger than R_c; the broken line is the coexistence curve of the paranematic and nematic phase for droplet with smaller radius (0.2 μm). (The temperature difference $T - T^*$ is given in Kelvins.) q is proportional to the surface-liquid crystal interaction potential g, *i.e.* $q = \frac{2}{9}\left(\frac{g}{S\sqrt{aL_1T^*}}\right)$. The material parameters used in the calculation are those of 5 CB. Its nematic-isotropic transition temperature in the bulk form is $T_c = T^* + 1.4\,\mathrm{K} \sim 34\,^\circ\mathrm{C}$.

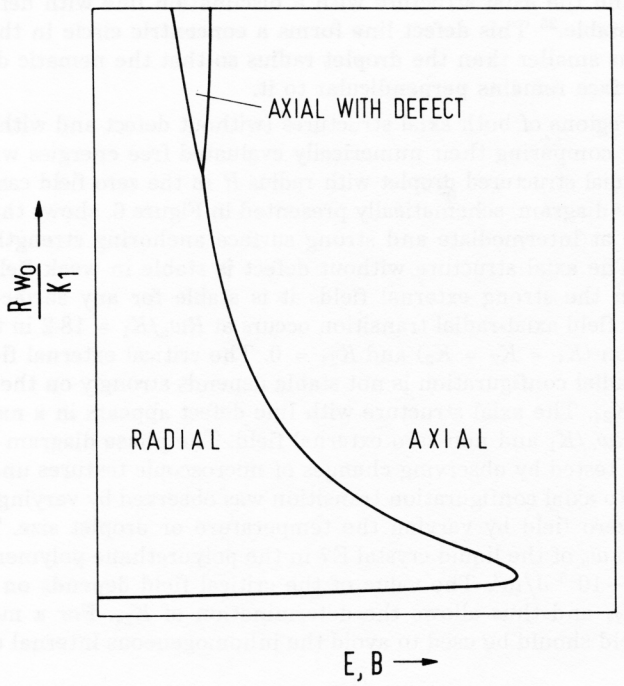

Figure 6. Schematic presentation of stability regions in the surface interaction-external field interaction plane for a spherical droplet with perpendicular anchoring at the wall.

Structural Phase Transitions – Spherical Droplets

The light scattering cross-section of nematic droplets, which is of basic importance for the operation of PDLC electrooptic devices (threshold voltage, response time, contrast ratio, *etc.*), strongly depends on the configuration of the director field. The phase transitions between different director configurations in the nematic phase are of structural type. The field or temperature induced transitions between different configurations are first order in contrast to the field induced transitions in planar systems (Freedericksz's) which are second order.

The bipolar configuration (Figure 2c), which takes place in PDLC materials where the polymer imposes tangential ordering of liquid crystal molecules at the surface, is relatively stable if the three Frank elastic constants K_i are comparable in magnitude. This is realized in most practical cases.

In the case of perpendicular boundary conditions at the wall, two stable nematic structures can be observed. The radial structure (Figure 2a) is stable only if the anchoring strength is strong or the droplet radius large enough. The axial structure (Figure 2b) is favorized if the anchoring strength is weak and the droplet sufficiently small or if there is an applied electric field of suitable strength.[24] In the limit of very weak anchoring the axial structures have no defects and the director field is nearly axial through the whole droplet. For stronger anchoring the deformation in the equatorial

region increases and the axial structure with a disclination line with defect strength 1/2 may become stable.[25] This defect line forms a concentric circle in the equatorial plane with a radius smaller than the droplet radius so that the nematic director field on the droplet surface remains perpendicular to it.

The stability regions of both axial structures (without defect and with line defect) are determined by comparing their numerically evaluated free energies with the total free energy of a radial structured droplet with radius R in the zero field case ($8\pi K_1 R$).[21] The phase stability diagram, schematically presented in Figure 6, shows that the radial structure is stable at intermediate and strong surface anchoring strengths but weak external fields.[25] The axial structure without defect is stable in weak fields for weak anchoring only. In the strong external fields it is stable for any surface anchoring strength. The zero field axial-radial transition occurs at $Rw_o/K_1 = 18.2$ in the one-constant approximation ($K_1 = K_2 = K_3$) and $K_{24} = 0$. The critical external field strength above which the radial configuration is not stable depends strongly on the ratio K_3/K_1 and on the value K_{24}. The axial structure with line defect appears in a narrow region at high values of Rw_o/K_1 and non-zero external field. The phase diagram has been so far experimentally tested by observing changes of microscopic textures under external field.[24] The radial to axial configuration transition was observed by varying the electric field, and in the zero field by varying the temperature or droplet size. The surface anchoring strength w_o of the liquid crystal E7 in the polyurethane polymer binder was determined to be $\sim 10^{-5}$ J/m^2. The value of the critical field depends on the surface elastic constant K_{24} and thus allows the determination of K_{24}. For a more detailed study, magnetic field should be used to avoid the inhomogeneous internal electric field effects.[25]

CYLINDRICAL MICROCAVITIES – RESULTS AND DISCUSSION

Phase transitions in liquid crystals confined into cylindrical cavities of supramicron size (glassy capillaries) arose great attention a long time ago particularly in connection to the stability of thread defects in the nematic phase.[26,27] Later, they were studied for the practical purpose of wave-guiding in nematic liquid crystal optical fibres.[16] The dielectric properties of the core which govern wave-guiding in such fibre depend on the nematic director field. The experiments on submicron cavities enabled the study of molecular anchoring at various solid surfaces.[28] The walls of opened cylindrical cavities are – in contrast to spherical droplets – accessible to preceeding chemical treatment for altering anchoring strengths and angles.

The configuration of a nematic liquid crystal in a cylindrical cavity is trivial under tangential boundary conditions, when all directions in the plane of the wall are equivalent. In this case the director is oriented everywhere parallel to the cylinder axis as this structure does not require any deformation energy. The interesting situation arises when the anchoring at the wall is homeotropic, *i.e.* when the molecules tend to orient perpendicular to the wall. Only phases and phase transitions for this case will be thus discussed in the following.

The Order-Disorder Phase Transition – Cylindrical Cavities

The order-disorder phase transition in cylindrical microcavities is expected to be similar to transitions in spherical and planar confinement. There is an early experimental study of Kuzma *et al.*[13] on the depression of T_c of the nematic liquid crystal

confined into cylindrical microchannels in a polycarbonate membrane. However, in that early study the effect of impurities introduced by the membrane has not been resolved from the effect due to elastic distortions caused by the small cylinder size. The theoretical study by Gartland *et al.*[20] illustrates the increase of ordering on approaching the transition temperature from above. Recently, a rather extensive NMR study of 5CB in polycarbonate membranes was carried out to examine the order and dynamics close to the surface in the paranematic phase.[28,29] The ^{2}H NMR spectra show a relatively large quadrupole splitting in this phase, which results from an ordered surface layer. The experimental data are consistent with the model where the order parameter S_0 in the first molecular layer of the liquid crystal in contact with the confining surface is nearly temperature independent. Such a behavior is expected when the dominant ordering interactions are local in nature. The constant order parameter $S_0 \sim 0.02$ in the first layer is followed by an exponential decay characterized by a coherence length which has a critical temperature dependence.

Structural Phase Transitions – Cylindrical Cavities

For the perpendicular molecular anchoring at the cavity wall there are three competing director field configurations:

Planar-radial configuration with the director field completely radial throughout the cylinder (Figure 7a) so that only splay deformation is present. The simple elastic theory can not describe the behaviour of the system close to the disclination line along

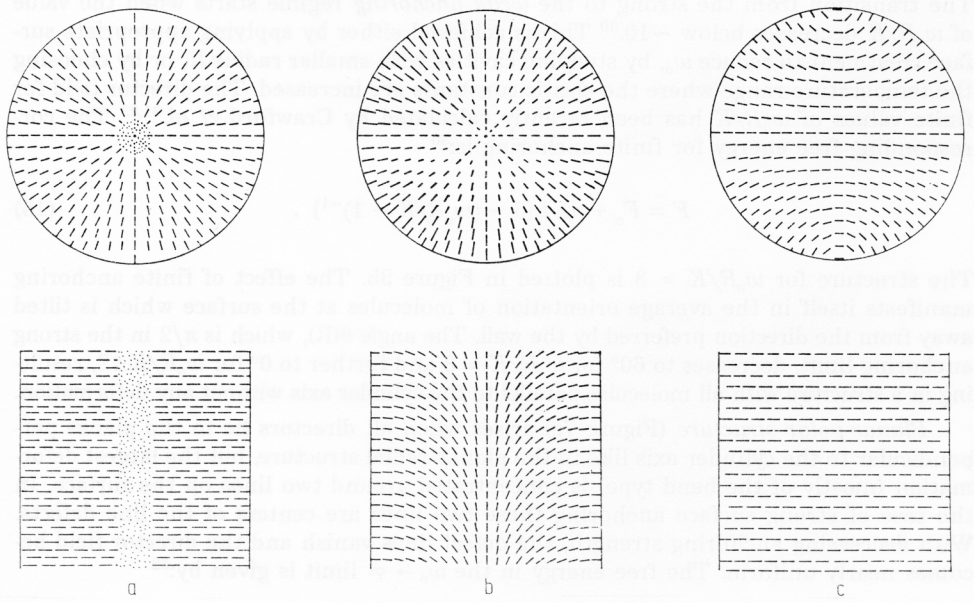

Figure 7. Schematic presentation (top and side cross-section) of three possible nematic liquid crystal configurations in cylindrical microcavity with preferred perpendicular alignment at the cavity wall: (a) planar-radial structure, (b) escaped-radial structure, (c) planar-polar structure.

the cylinder axis. Therefore an isotropic core with radius r_0 is introduced to avoid the singular behavior of the elastic free energy. In the one-elastic-constant-approximation ($K_1 = K_2 = K_3 = K$) the free energy of the liquid crystal in this configuration is:[1]

$$F = F_0 + \pi KL \ln R/r_0 + F(core) \ . \tag{12}$$

Here R denotes the cylinder radius and L its length.

Escaped-radial structure with the director containing both radial and axial components (Figure 7b). The director which is perpendicular to the wall close to it bends away to become parallel to the cylinder axis in the center. This arrangement has a continuous director field and involves no isotropic core. It was observed optically in capillaries of size ~200 μm (Figure 8). The spatial dependence of the angle $\theta(\vec{r})$ between the director and cylinder axis was determined by Cladis *et al.*[26,27] for the *strong anchoring case* (Figure 9a), where the molecular orientation on the cavity wall is strictly perpendicular, *i.e.* for $w_0R/K \to \infty$ and $\theta(R) = \pi/2$, as:

$$\theta(r) = 2 \tan^{-1}(r/R) \tag{13}$$

in the one elastic constant approximation. The corresponding F is:

$$F = F_0 + 3\pi KL \ . \tag{14}$$

The transition from the strong to the *weak anchoring* regime starts when the value of w_0R/K decreases below ~10.[30] This is achieved either by applying appropriate surface treatment to reduce w_0, by studying cavities with smaller radius R, or by choosing the temperature range where the elastic constants are increased. The director field for finite values of w_0R/K has been recently calculated by Crawford *et al.*[31,32] The corresponding free energy for finite anchoring is:[30]

$$F = F_0 + \pi KL[3 - (w_0R/K - 1)^{-1}] \ . \tag{15}$$

The structure for $w_0R/K = 3$ is plotted in Figure 9b. The effect of finite anchoring manifests itself in the average orientation of molecules at the surface which is tilted away from the direction preferred by the wall. The angle θ(R), which is $\pi/2$ in the strong anchoring limit, decreases to 60° for $w_0R/K = 3$ and further to 0° for $w_0R/K \leq 2$, resulting in a structure with all molecules parallel to the cylinder axis without any deformation.

Planar-polar structure (Figure 7c) arises when all directors lie in the planes perpendicular to the cylinder axis like in the planar-radial structure, but the largest deformation (mostly of the bend type) is concentrated around two lines on the surface. In the case of strong surface anchoring these two lines are centers of the line defects. With decreasing anchoring strength, the defect lines vanish and the director field becomes nearly uniform. The free energy in the $w_0 \to \infty$ limit is given by:[32]

$$F = F_0 + \pi KL \ln(R/2r_0) \ , \tag{16}$$

where the radius of the defect lines, r_0, is of the order of molecular dimension.

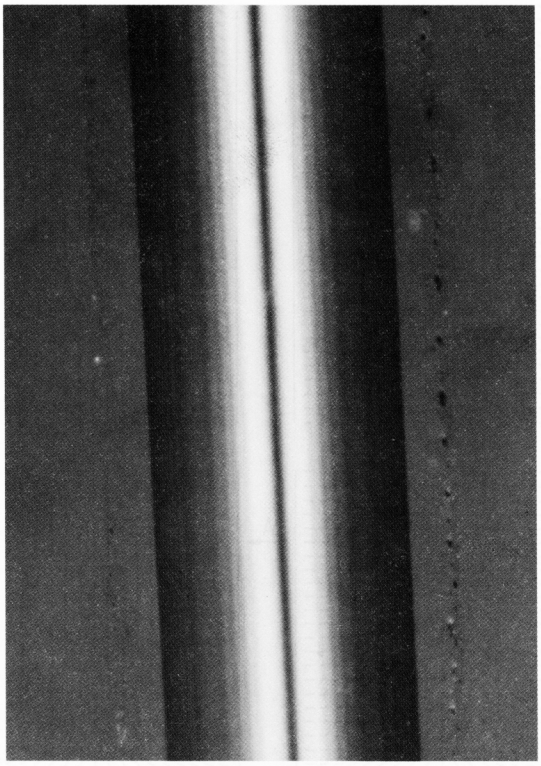

Figure 8. A polarizing-microscope photograph of the escaped-radial structure in a cylindrical capillary tube with radius 200 μm made at the Liquid Crystal Institute, Kent State University, Kent, Ohio, by G. Crawford.

Each of the three director configurations described above corresponds to a relative minimum in the free energy. Direct mutual comparison shows that the free energy of the escaped-radial structure is the lowest unless the cylinder radius R is well below 1μm. The planar-polar and planar-radial structures are thus limited to small cylinder sizes. The free energy of the planar-polar configuration is the lower one if $K_1 \approx K_3$ and $w_o R/K <\sim 5$. The transition from the escaped-radial into the planar-polar structure has been experimentally observed by diminishing the cylinder size.[32] The planar-radial configuration could occur only for $K_1 \ll K_3$, which is the case close to the transition of the nematic into the smectic A phase.

In most practical cases, however, the monodomain escaped radial structure is not realized. Intrinsic fluctuations at the phase transition from the isotropic into the nematic phase and the irregularities of the cylinder wall lead to a series of alternating radial (R) and hyperbolic (H) point defects along the cylinder symmetry axis[30,33] as both directions of the bend deformation, »up« and »down«, are energetically equivalent (Figure 9c). In order to stimulate these defect structures the free energy of a monodomain with a finite length L, incorporating half of the radial and half of the hyperbolic defect, must be considered.[30] The calculation shows that such structure is

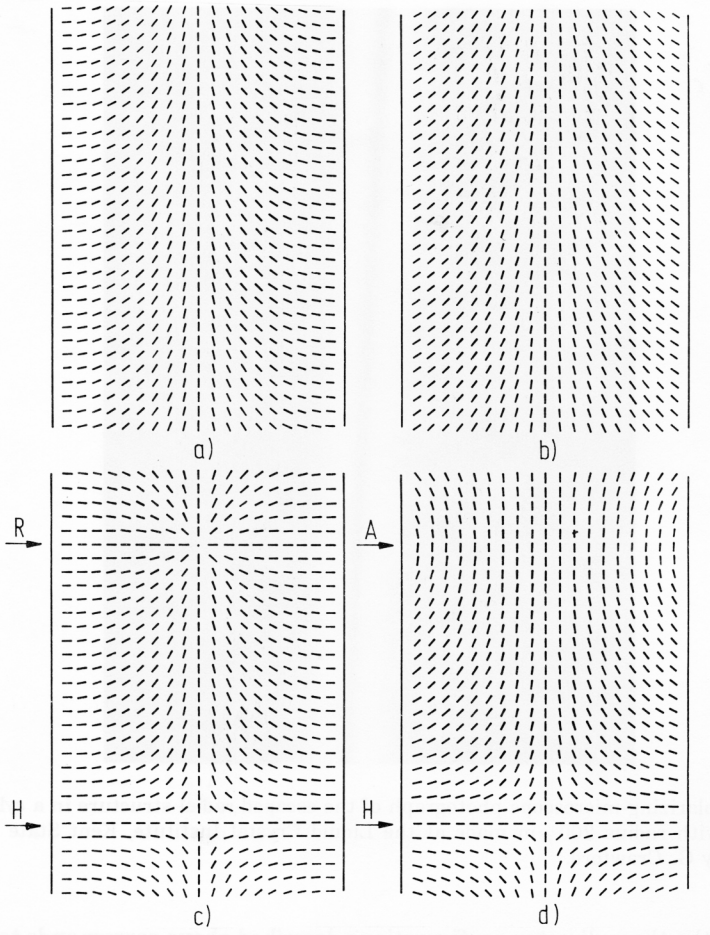

Figure 9. Four possible variations of the escaped-radial structure, which takes place in large cylindrical cavities with perpendicular boundary conditions (after Ref. 30): (a) monodomain escaped-radial structure in the strong anchoring limit ($w_oR/K \to \infty$); (b) monodomain escaped-radial structure for $w_oR/K = 3$; (c) escaped-radial structure with a radial (R) and a hyperbolic (H) defect in the strong anchoring limit; (d) escaped-radial structure with an axial wall (A) and a hyperbolic (H) defect for $w_oR/K = 3$.

stable in the strong anchoring limit for defect separation $L > \sim 0.25\ R$. If defects are closer than $L_o = 0.25\ R$, the attraction causes their annihilation, whi e for $L > L_o$ the repulsion between the neighbouring defects stabilizes a periodic array of equally sized ($L > L_o$) oppositely oriented domains.

In the transition region from the strong to the *weak anchoring* regime, a different defect structure can appear with only hyperbolic defects while the radial defects are substituted by defectless, predominantly axial director field (Figure 9d). The transition from the defect structure with alternating radial and hyperbolic defects to the struc-

ture with only hyperbolic defects is first order. The latter structure is generally the more stable when $w_o R/K \leq 5$. The exception is the region $0.25 \leq L/R \leq 2$ where the occurence of the transition strongly depends on the value of L/R.

CONCLUSIONS

Recent increasing interest in basic physics and application of microconfined nematic liquid crystals stimulated us to summarize a few basic results in this review. In particular, the liquid crystal symmetry breaking in spherical and cylindrical confinement is treated. For the submicron size confinement, the Landau-de Gennes theory is used to describe the order-disorder transitions between the nematic and isotropic (paranematic) phase. The effects of the surface and deformation on the inhomogeneous ordering in the nematic, boundary-layer nematic, and paranematic phase are illustrated. For the supramicron size droplets and cylinders, the description based on the Frank elastic free energy is used to describe the transitions of the Freedericksz type. These transitions can be either field- or temperature-induced. It is shown that the stability regions of different structures strongly depend on liquid crystal elastic constants and on the type and strength of the anchoring of liquid crystal molecules on the confining surface. The corresponding phase diagrams are presented and their potential use for the determination of the relevant material constants is emphasized. The importance of these structures and field-induced transitions for the understanding of optical shutters operation, based on PDLC materials, is the main driving force in the research of microconfined liquid crystals.

Acknowledgement. – The authors thank Dr. I. Vilfan, Dr. S. Kralj, and Dr. G. Crawford for their help in the preparation of this review.

REFERENCES

1. P. G. de Gennes, *The Physics of Liquid Crystals*, Clarendon Press, Oxford 1974.
2. E. B. Priestley, P. J. Wojtowicz, and P. Sheng, *Introduction to Liquid Crystals*, Plenum Press, New York and London 1974.
3. L. D. Landau and E. M. Lifshitz, *Statistical Physics*, Pergamon Press, Oxford 1969.
4. P. G. de Gennes, in *Liquid Crystals 3*, Eds. G. H. Brown and M. M. Labes, Gordon and Breach, London and New York 1972.
5. P. Sheng, *Phys. Rev.* **A3** (1982) 1610.
6. A. Poniewierski and T. J. Sluckin, *Mol. Phys.* **55** (1985) 1113;
   A. Poniewierski and T. J. Sluckin, *Liq. Cryst.* **2** (1987) 281.
7. V. Feedericksz and V. Zolina, *Trans. Far. Soc.* **29** (1933) 919.
8. J. W. Doane, N. A. Vaz, B. G. Wu, and S. Žumer, *Appl. Phys. Lett.* **48** (1986) 269.
9. J. L. West, *Mol. Cryst. Liq. Cryst.* **157** (1988) 427.
10. J. W. Doane, A. Golemme, J. L. West, J. B. Whitehead, and B. G. Wu, *Mol. Cryst. Liq. Cryst.* **165** (1988) 511.
11. J. W. Doane, *Material Research Science Bulletin* **16** (1991) 22.
12. J. W. Doane, in *Liquid Crystals: Applications and Uses*, Ed. B. Bahadur, World Scientific, New York 1990.
13. M. Kuzma and M. M. Labes, *Mol. Cryst. Liq. Cryst.* **100** (1983) 103.
14. G. P. Crawford, M. Vilfan, J. W. Doane, and I. Vilfan, *Phys. Rev.* **A43** (1991) 835.
15. A. Pargellis, N. Turok, and B. Yurke, *Phys. Rev. Lett.* **67** (1991) 1570.
16. P. Palffy-Muhoray, M. D. Lee, and J. L. West, *Mol. Cryst. Liq. Cryst.* **179** (1990) 445.
17. R. A. Hikmet, *J. Appl. Phys.* **68** (1990) 4406.
18. R. Stannarius, G. P. Crawford, L. C. Chien, and J. W. Doane, *J. Appl. Phys.* **70** (1991) 135.

19. I. Vilfan, M. Vilfan, S. Žumer, *Phys. Rev.* **A 40** (1989) 4724.
20. E. C. Gartland, Jr., P. Palffy-Muhoray, R. S. Varga, *Mol. Cryst. Liq. Cryst.* **199** (1991) 429.
21. S. Kralj, S. Žumer, and D. W. Allender, *Phys. Rev.* **A 34** (1991) 2943.
22. A. Golemme, S. Žumer, D. W. Allender, and J. W. Doane, *Phys. Rev. Lett.* **61** (1988) 2937.
23. J. W. Doane, *Magnetic Resonance of Phase Transitions*, Chapter 4, Academic Press, New York 1979.
24. J. H. Erdmann, S. Žumer, and J. W. Doane, *Phys Rev. Lett.* **64** (1990) 19.
25. S. Žumer, S. Kralj, and J. Bezič, *Proc. ECLC Conference*, Courmayeur 1991.
26. P. E. Cladis and M. Kleman, *J. Phys* (Paris) **33** (1972) 591.
27. R. B. Meyer, *Phylosoph. Mag.* **27** (1973) 405.
28. G. P. Crawford, R. Stannarius, and J. W. Doane, *Phys. Rev.* **44** (1991) 2558.
29. G. P. Crawford, D. K. Yang, S. Žumer, D. Finotello, and J. W. Doane, *Phys. Rev. Lett.* **66** (1991) 723.
30. I. Vilfan, M. Vilfan, and S. Žumer, *Phys. Rev.* **A 43** (1991) 6875.
31. G. P. Crawford, D. W. Allender, J. W. Doane, M. Vilfan, I. Vilfan, *Phys. Rev.* **A44** (1991) 2570.
32. D. W. Allender, G. P. Crawford, and J. W. Doane, *Phys. Rev. Lett.* **67** (1991) 1442.
33. L. Williams, P. Pieranski, P. E. Cladis, *Phys. Rev. Lett.* **29** (1972) 90.

SAŽETAK

Fazni prijelazi u mikrokonfiniranima nematičkim tekućim kristalima

M. Vilfan i S. Žumer

Dan je kratki prikaz stabilnih faza i faznih prijelaza u nematičkim tekućim kristalima konfiniranima u šupljine reda veličine mikrometra (mikrokonfinirani tekući kristali). Pojave konfinacije pri različitim interakcijama površina–tekući kristal proučavane su za šupljine sfernog i cilindričnog oblika. Fazni su prijelazi ili tipa red-nered, kada se mijenja veličina parametra uređenosti, ili strukturnog tipa, između različitih konfiguracija polja nematičkog usmjeravajućeg polja.